ISSN 1068-3356, Bulletin of the Lebedev Physics Institute, 2022, Vol. 49, No. 10, pp. 322–328. © Allerton Press, Inc., 2022.
Russian Text © The Author(s), 2022, published in Kratkie Soobshcheniya po Fizike, 2022, Vol. 49, No. 10, pp. 25–34.

Geant4 Simulation of the Effect of Cherenkov Radiation Cone Transformation in the X-ray Region

I. A. Kishin[a,b,*], V. I. Dronik[a], A. S. Kubankin[a,b], R. M. Nazhmudinov[a,b], and V. S. Sotnikova[a,c]

[a] *Belgorod National Research University, Belgorod, 308015 Russia*

[b] *Lebedev Physical Institute, Russian Academy of Sciences, Moscow, 119991 Russia*

[c] *Belgorod State Technological University named after V.G. Shukhov, Belgorod, 308012 Russia*

**e-mail: ivan.kishin@mail.ru*

Received April 13, 2022; revised April 17, 2022; accepted April 17, 2022

Abstract—In this paper, we present the simulation results of Cherenkov radiation in the soft X-ray range using the GEANT4 software package. The effect of Cherenkov radiation cone transformation is demonstrated.

Keywords: Cherenkov radiation, GEANT4, relativistic electrons, soft X-ray source

DOI: 10.3103/S1068335622100037

1. INTRODUCTION

As is known, Cherenkov radiation (CR) is formed when the charged particle velocity in a transparent medium becomes above the light phase velocity in this medium, i.e., the condition $n > 1/\beta$, $\beta = v/c$ should be satisfied. Here, n is the refractive index, v is the charged particle velocity, and c is the light speed in vacuum. In the visible spectral range, CR is well studied theoretically and experimentally; based on CR, charged particle detectors are developed for identifying and determining particle energies in accelerator beams.

The CR existence in the X-ray region was considered to be impossible. In 1976, it was shown [1] that CR with an energy of ~250 eV can be generated in narrow spectral ranges due to the resonant behavior of the refractive index at photoabsorption edges.

Later, the possibility of CR generation in the X-ray region was experimentally confirmed by several groups [2, 3]. Interest in CR in the X-ray region is caused by its quasi-monochromatic spectrum and high spectral density. These properties make it possible to consider the CR mechanism applicability to new sources of soft X-rays in the carbon transmission window range [4, 5]. One of the obstacles for developing such sources is the low angular radiation density caused by large apex angles of the Cherenkov cone. One of the solutions of this problem is the use of the sliding interaction of emitting particles with the target surface plane [6, 7]. In this geometry, the particle path length in a material increases; hence, the number of generated photons increases. Furthermore, the effect of CR cone transformation [7] was predicted, which is implemented in the case where the sliding angle becomes less than the angle between the generatrix and CR cone axis. In this case, the radiation cone narrows, and the radiation angular density significantly increases. The effect of CR cone transformation was considered in the case of a charged particle emission from a semi-infinite target [7] and in the case of an electron emission from a material layer [8].

CR in the X-ray region near photoabsorption lines was simulated using the Geant4 software package [9] which represents a platform for simulating physical processes based on Monte Carlo method. Previously, the Geant4 platform applicability to CR simulation in the X-ray region [10] was demonstrated, the consistency of simulation results with theoretical calculations by the polarization current model was shown [11].

In this paper, we present the results of the study of CR in the X-ray region, generated by an electron beam passed through a material layer. The effect of the target geometry on the CR yield is demonstrated. The previously predicted effect of the CR cone transformation was shown for carbon and aluminum targets [7].

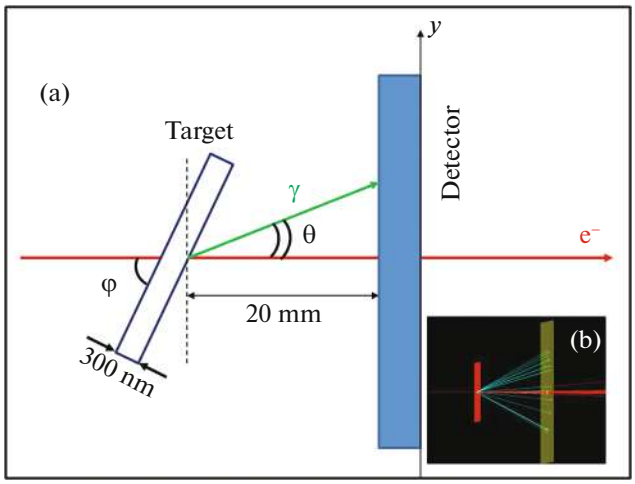

Fig. 1. (a) Experimental geometry: γ is the CR propagation directions, e^- is the electron beam propagation direction, θ is the "Cherenkov" angle, φ is the target orientation angle. (b) Model visualization window in the Geant4.

2. SIMULATION GEOMETRY

To study CR in the Geant4, a model of irradiation of thin targets (25 × 25 mm in size and 300 nm thick) by an electron beam with an energy of 7 MeV at various angles in the range from 3° to 90° was developed. The simulation geometry and visualization window of the model in the Geant4 is shown in Fig. 1. The electron beam with an energy of 7 MeV is incident on the target at an angle φ. The beam interaction with the target generates CR which propagates from the target at a "Cherenkov" angle θ and is recorded by a virtual detector placed at a distance of 20 mm from the target. In the simulation, it was supposed that the target, electron source, and X-ray detector are placed in a common vacuum volume. The photon detection efficiency of the detector is 100%. For an accurate analysis, all processes generating electromagnetic radiation, e.g., bremsstrahlung or transition radiation, were disabled in the simulation, except for CR.

3. SIMULATION PARAMETERS

One of the parameters used in the CR simulation in the Geant4 is the material refractive index (see Table 1) determined using a real part of the scattering factor depending on the photon energy [12].

Figure 2 shows the calculated refractive indices for carbon near the absorption K-edge and aluminum near the absorption L-edge.

Figure 2 shows that there exists a region in which the refractive index becomes more than unity; for carbon this region is from 281.5 to 286.7 eV, for aluminum, from 64.8 to 98.8 eV. In these spectral regions, the condition $n > 1/\beta$ is satisfied; hence, CR can be generated.

The next parameter affecting the radiation yield is the photoabsorption length in material ($L_{abs} = 1/\mu\rho$, where μ is the linear attenuation factor and ρ is the material density), characterizing the photon absorption process in a target material, which is also considered in the simulation.

The photoabsorption lengths in the region of soft X-rays from 20 to 350 eV for carbon and aluminum are shown in Fig. 3. The real part of the scattering factor and attenuation factors were taken for calculations from the Henke database [13].

Table 1. Characteristics of materials used in the simulation

Target material	Photoabsorption edge	Density, g/cm^3	Photon energy ω_{max}, eV	Cherenkov angle, deg	n for ω_{max}
Carbon	K	3.51	284	4.85	1.0059
Aluminum	L_{III}	2.7	72.5	15.28	1.0354

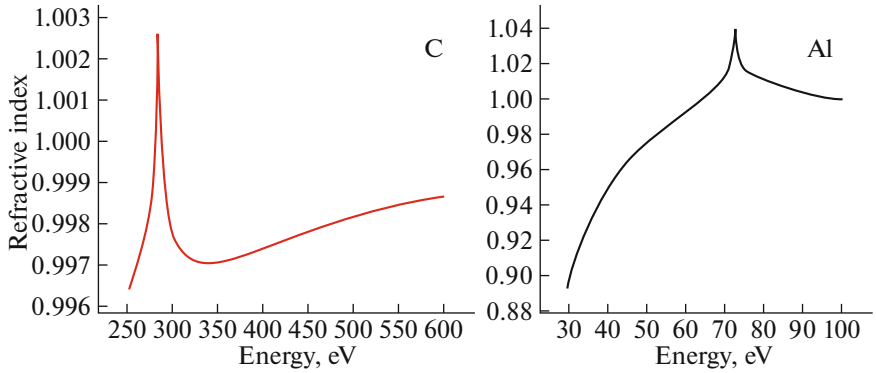

Fig. 2. Refractive indices for carbon (red curve) and aluminum (black curve).

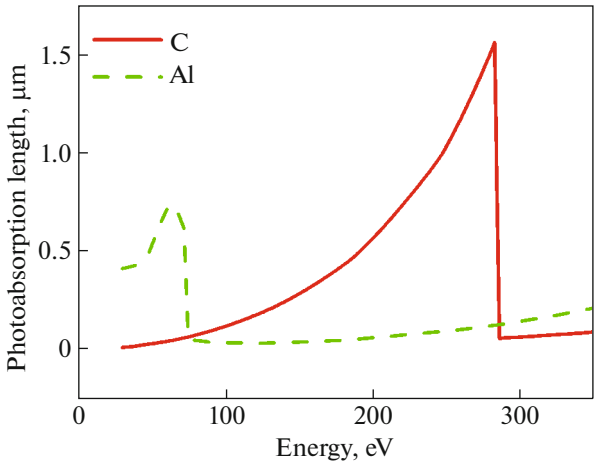

Fig. 3. Carbon (diamond) (red curve) and aluminum (green curve) photoabsorption lengths.

4. CR SIMULATION IN THE GEANT4

To observe the effect of CR cone transformation, the electron beam incidence on the target was simulated for various angles. Figure 4 shows the CR energy spectrum obtained in the simulation of the interaction of the 7-MeV electron beam with carbon and aluminum targets for the various target orientation angles: 3°, 5°, 7°, 15°, 45°, and 90°. The CR yield maximum is observed at the energy of ~284 and 72 eV for carbon and aluminum targets, respectively.

The obtained full widths at half-maximum (FWHM) of spectral lines in the simulation are listed in Table 2. It may be noted that full widths at half-maximum do not exceed 1 eV for the carbon target and 2.5 eV for the aluminum target for all electron beam incidence angles, which shows the CR spectrum monochromaticity.

Figures 5 and 6 show the thermal maps of the angular distributions of recorded photons in the detector. We can see that the CR shifts to the beam axis as the electrons incidence angle decreases. When the elec-

Table 2. Full widths at half-maximum of spectral lines (eV)

Target material	Angle φ					
	3°	5°	7°	15°	45°	90°
Carbon	0.84	0.82	0.90	0.86	0.84	0.68
Aluminum	1.95	2.25	2.40	3.0	2.10	1.95

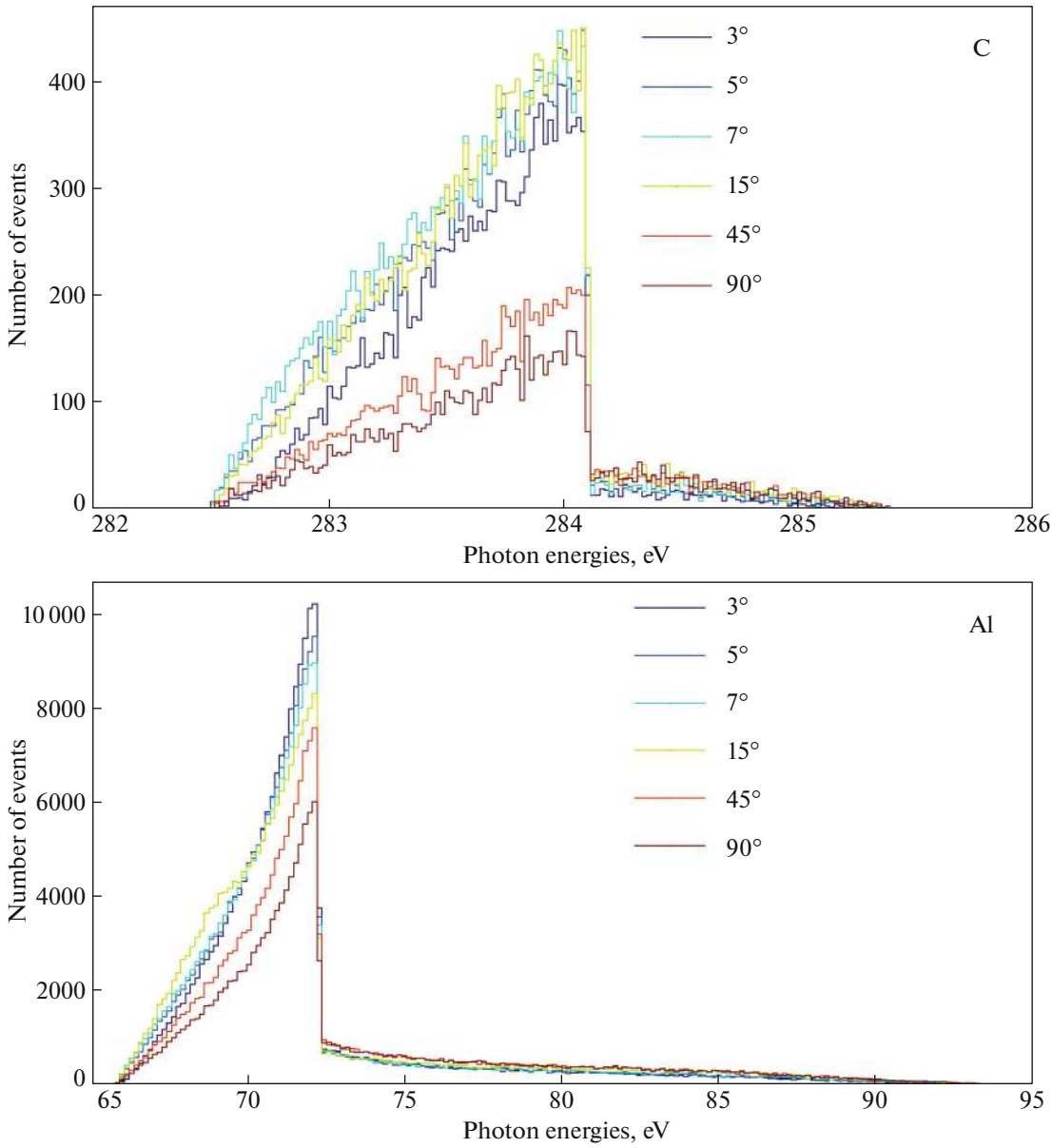

Fig. 4. CR spectra from carbon and aluminum targets taking into account photoabsorption.

tron incidence angle becomes smaller than the "Cherenkov" angle (see Table 1), the angular radiation density increases; this phenomenon is called the CR cone transformation [7].

Figure 7 shows the transverse profiles of the CR angular distribution at $\xi = 0$; these results show an increase in the angular radiation density and photon shift to the central beam axis with decreasing the electron incidence angle.

To quantitatively estimate the CR yield, the integration region enclosed by a rectangle in Figs. 5 and 6 was chosen. This region has an angular size of 12° × 6° for carbon and 7° × 14° for aluminum.

The summed number of photons was divided into the number of electrons (10^8 particles) passed through the target. The result obtained is shown in Fig. 8.

Thus, it is shown demonstrated that the angular radiation density increases with decreasing electron incidence angle on the target; the maximum value is at the incidence angle of 3°. The number of photons in the selected area at incidence angles of 90° and 3° differs by a factor of 25.7 for carbon and by a factor of 9.0 for aluminum.

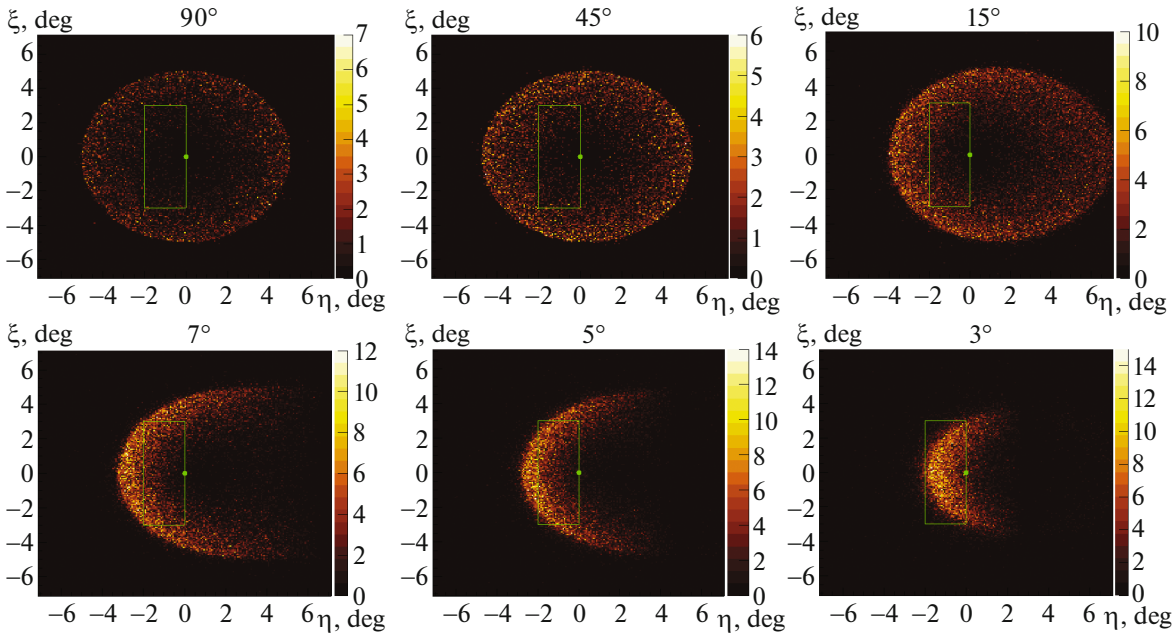

Fig. 5. Thermal maps of the distribution of radiation from the carbon target as functions of the incidence angle of the electron beam on the target. The number of incident particles is 10^8.

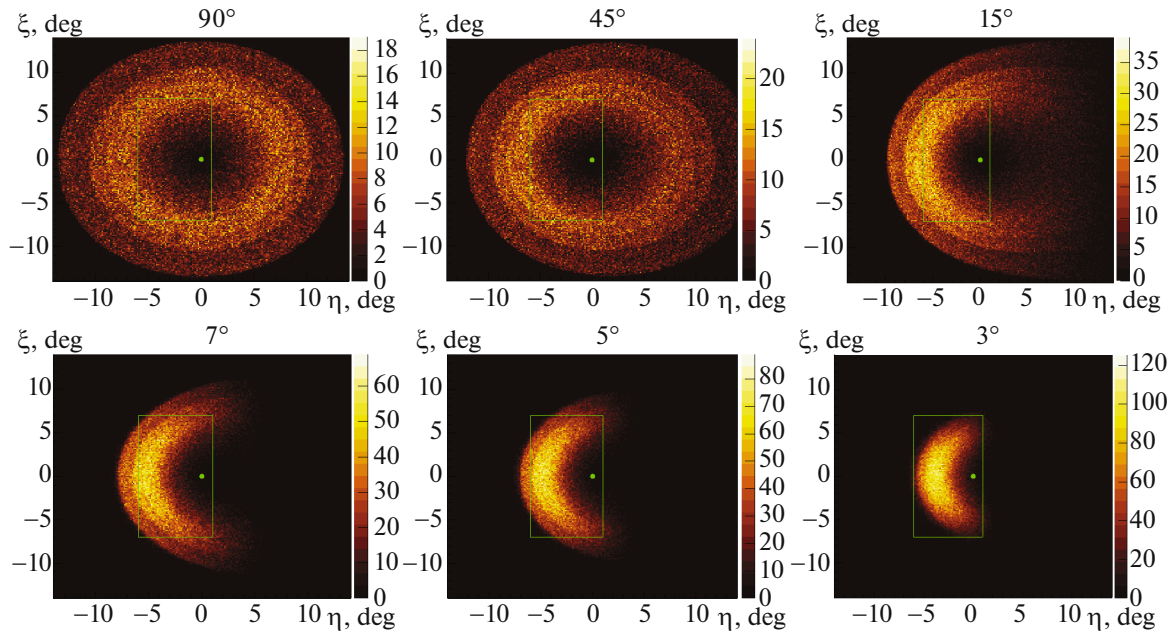

Fig. 6. Thermal maps of the distribution of radiation from the aluminum target as functions of the incidence angle of the electron beam on the target. The number of incident particles is 10^8.

CONCLUSIONS

(i) CR was simulated in the Geant4 software package for various target types at the electron beam energy of 7 MeV. It was shown that the energy spectrum maximum corresponds to the photoabsorption edge energy. The beam energy was chosen to make possible the experiment on the microtron of the "Pakhra" accelerator complex using the "Rentgen-1" setup intended for low-background studies of X-ray radiation [14, 15].

(ii) The effect of CR cone transformation is demonstrated. It was found that the maximum photon yield is at the electron incidence angle on the target smaller than the "Cherenkov" angle.

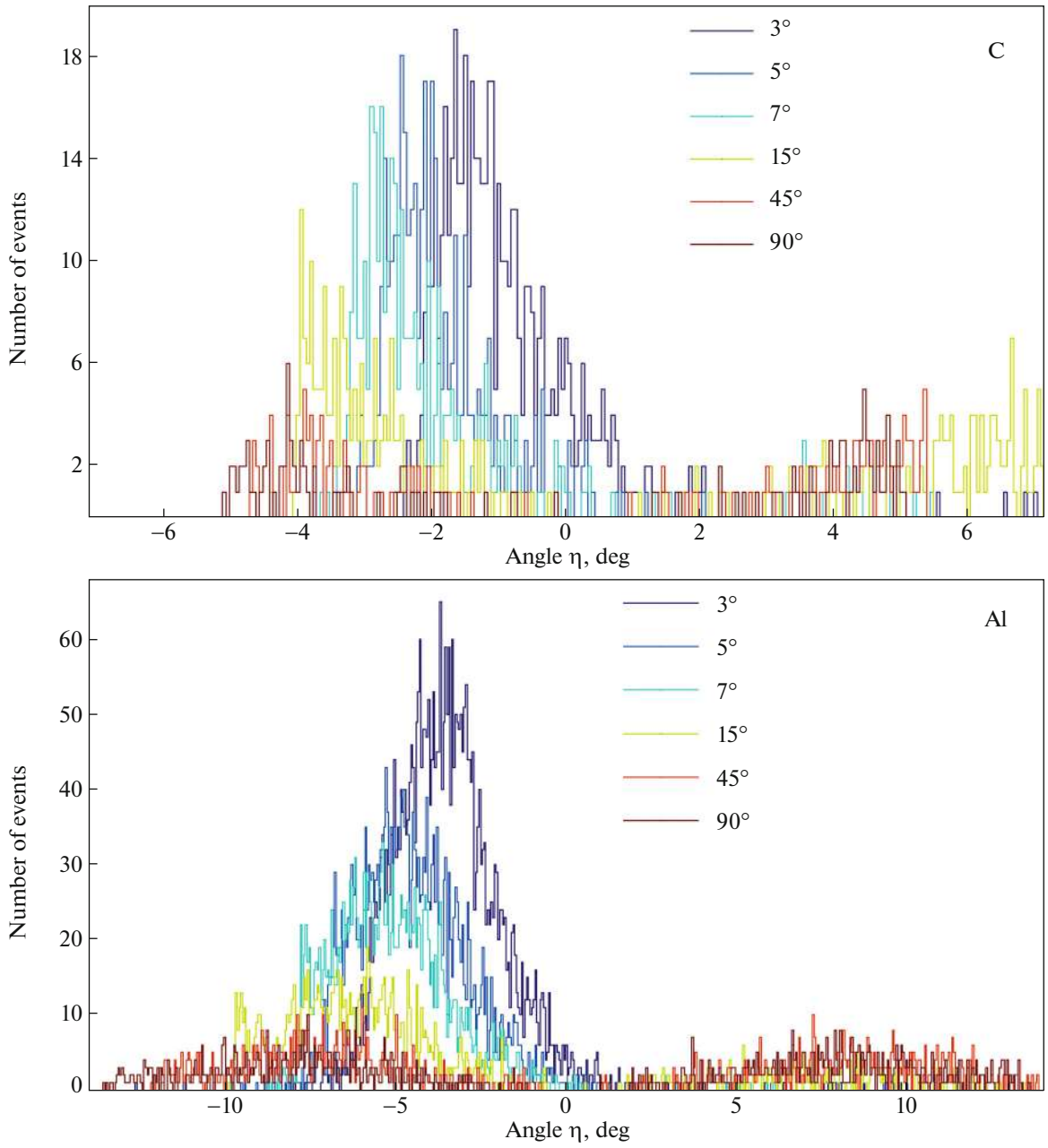

Fig. 7. Angular distribution of CR from carbon and aluminum targets for various angles φ from 3° to 90°.

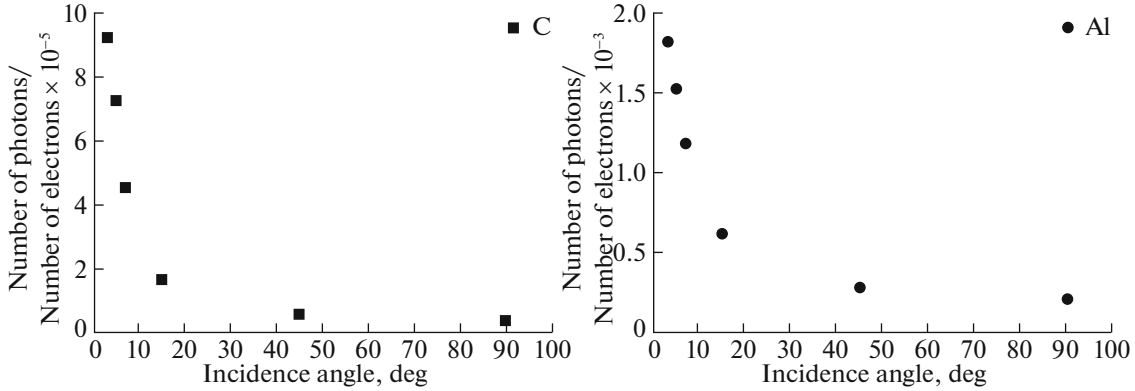

Fig. 8. Number of CR photons formed in carbon and aluminum targets as a function of the angle φ.

(iii) The presented simulation results in combination with the experimental [4, 5] and theoretical [6, 8] data can be used to develop an intense CR source of soft X-rays in energy ranges from 70 to 300 eV.

FUNDING

This work was financially supported by a Program of the Ministry of Education and Science of the Russian Federation for higher education establishments, project No. FZWG-2020-0032 (2019–1569). The work was carried out with the support of a grant from the President of the Russian Federation for young scientists – candidates of science MK-1320.2022.1.2.

CONFLICT OF INTEREST

The authors declare that they have no conflicts of interest.

REFERENCES

1. Bazylev, V.A., Glebov, V.I., Denisov, E.I., Zhevago, N.K., and Khlebnikov, A.S., Čerenkov radiation as an intense x-ray source, *JETP Lett.*, 1976, no. 24, pp. 371–374. http://jetpletters.ru/ps/1814/article_27732.pdf.
2. Bazylev, V.A., Glebov, V.I., Denisov, E.I., Zhevago, N.K., Kumakhov, M.A., Khlebnikov, A.S., and Tsinoev, V.G., X-ray Čerenkov radiation. Theory and experiment, *Sov. Phys. JETP*, 1981, vol. 54, no. 5, pp. 884–892. http://jetp.ras.ru/cgi-bin/dn/e_054_05_0884.pdf
3. Moran, M.J., Chang, B., Schneider, M.B., and Maruyama, X.K., Grazing-incidence Cherenkov X-ray generation, *Nucl. Instrum. Methods B*, 1990, vol. 48, nos. 1–4, pp. 278–290. https://doi.org/10.1016/0168-583X(90)90124-D
4. Knulst, W., van der Wiel, M.J., Luiten, O.J., and Verhoeven, J., High-brightness, narrowband, and compact soft x-ray Cherenkov sources in the water window, *Appl. Phys. Lett.*, 2003, vol. 83, pp. 4050–4052. https://doi.org/10.1063/1.1625999
5. Kaplan, A.E. and Shkolnikov, P.L., Radiation efficiency of water-window Cherenkov sources using atomic-shell resonances, *Appl. Phys. Lett.*, 2005, vol. 86, p. 024107. https://doi.org/10.1063/1.1850190
6. Zhevago, N.K. and Glebov, V.I., X-ray Cherenkov radiation at grazing incidence of electrons, *Phys. Lett. A*, 1991, vol. 160, no. 6, pp. 564–570. https://doi.org/10.1016/0375-9601(91)91069-P
7. Gary, C., Kaplin, V., Kubankin, A., Nasonov, N., Piestrup, M., and Uglov, S., An investigation of the Cherenkov X-rays from relativistic electrons, *Nucl. Instrum. Meth. Phys. Res. B*, 2005, vol. 227, pp. 95–103. https://doi.org/10.1016/j.nimb.2004.06.015
8. Kishchin, I.A., Kubankin, A.S., Nikulicheva, T.B., Al-Omari, M., Sotnikov, A.V., and Starovoitov, A.S., Effect of Vavilov-Cherenkov radiation cone transformation upon entry of a relativistic electron into a substance layer, *Phys. At. Nucl.*, 2016, vol. 79, no. 13, pp. 1560–1564. https://doi.org/10.1134/S1063778816130044
9. GEANT4 collaboration, *GEANT4 Physics Reference Manual Release 10.7*, CERN, 2020.
10. Alekseev, B.A., Shevelev, M.V., and Kon'kov, A.S., Simulation of Cherenkov X-rays in the GEANT4 near aluminum absorption edges, Preprint of ResearchGate, 2020. https://doi.org/10.13140/RG.2.2.18109.20960
11. Shevelev, M., Konkov, A., and Alekseev, B., Spectral and polarization characteristics of X-ray hybrid radiation, *Nucl. Instrum. Methods Phys. Res. B*, 2020, vol. 464, no. 1, pp. 117–122. https://doi.org/10.1016/j.nimb.2019.12.010
12. Knulst, W., Cherenkov radiation in the soft X-ray region: Towards a compact narrowband source, *PhD Dissertation*, Eindhoven: Eindhoven University of Technology, 2004. http://alexandria.tue.nl/extra2/200410462.pdf.
13. Henke, B., Gullikson, E., and Davis, J., X-ray interactions: Photoabsorption, scattering, transmission, and reflection at E = 50-30000 eV, Z = 1-92, *Atom. Data Nucl. Data*, 1993, vol. 54, no. 2, pp. 181–342. https://doi.org/10.1006/adnd.1993.1013
14. Alekseyev, V.I., Astapenko, V.A., Eliseyev, A.N., Irribarra, E.F., Karpov, V.A., Kishin, I.A., Krotov, Y.A., Kubankin, A.S., Nazhmudinov, R.M., Al-Omari, M., and Sakhno, S.V., Investigation into the mechanisms of X-ray generation during the interaction between relativistic electrons and a medium by means of the Röntgen-1 setup, *J. Surf. Invest.: X-ray, Synchrotron Neutron Tech.*, 2017, vol. 11, no. 4, pp. 694—698. https://doi.org/10.1134/S1027451017040036
15. Alekseev, V.I., Eliseev, A.N., Kishin, I.A., Klyuev, A.S., Kubankin, A.S., and Nazhmudinov, R.M., Effect of the grain size of powder targets on the spectra of parametric x-ray radiation of relativistic electrons, *Bull. Lebedev Phys. Inst.*, 2021, vol. 48, no. 2, pp. 35–40. https://doi.org/10.3103/S1068335621020056

Translated by A. Kazantsev